



Original Article

Potential Therapeutic Effect of TLR4-Primed Mesenchymal Stem Cells in Lessening Kidney Damages in Rat Model of Diabetic Nephropathy

Mohammad Tollabi¹ Ph.D., Navid Ghasemzadeh² Ph.D.,
Ali Dehghani Firoozabadi^{3*} Ph.D.

¹ Department of Tissue Engineering and Regenerative Medicine, Faculty of Advanced Technologies in Medicine, Iran University of Medical Sciences, Tehran, Iran

² Department of clinical Biochemistry and applied cell sciences, Faculty of Medicine, Urmia University of Medical Sciences, Urmia, Iran

³ Yazd Cardiovascular Research Center, Non-communicable Diseases Research Institute, Shahid Sadoughi University of Medical Sciences, Yazd, Iran

ABSTRACT

Article history

Received: 24 Aug 2021

Accepted: 9 Sep 2022

Available online: 15 Oct 2022

Keywords

Diabetic nephropathy

Inflammation

Mesenchymal stem cells

TLR4 priming

Background and Aims: Substantial damage to the kidney tissue and diabetic nephropathy (DN) can be caused by chronic hyperglycemic conditions and exposure to a high level of blood glucose. In the current study, we explored the capability of adipose-derived mesenchymal stem cells (ADSCs) and Toll-like receptor-4-primed mesenchymal stem cells (TLR4-primed MSCs) on kidney regeneration, resolution of inflammation, and alleviation of diabetic nephropathy in DN in the rats.

Materials and Methods: STZ-induced diabetic rat models were divided into 5 subgroups, including 1) DN group, 2) DN group received insulin, 3) DN group received human foreskin fibroblast (DN-HFF), 4) DN group received single pulse of 1×10^6 cells of MSCs and 5) DN group received single pulse of TLR4-primed MSCs. Thereafter, biochemical and histological analysis was performed on DN-model groups. Biochemical analysis exhibited a blood urea nitrogen level recovery in both MSCs and TLR4-primed MSCs-treated groups. Administration of MSCs also up-regulated mRNA expression of Bcl-xL, while the expression of Bax was significantly down-regulated.

Results: Histological and molecular results showed that TLR4-primed MSCs have an anti-inflammatory and anti-apoptotic effect on inflamed kidneys and effectively reduced DN indicators in the TLR4-primed MSCs group compared to the unprimed MSCs group.

Conclusion: Priming with LPS improves the therapeutic effects of MSCs in the rat model of DN, consequently lessening the symptoms of DN rats. This study proposes that primed MSCs can be served as a potential therapeutic approach in diabetes mellitus and DN management.

Introduction

Diabetes mellitus is a metabolic disease considered by elevated blood glucose due to impaired insulin homeostasis and lead to the development of microvascular complications. Prolonged hyperglycemia and chronic inflammation lead to sustained damage to small blood vessels in various organs, especially blood vessels of the kidney [1]. Diabetic nephropathy (DN) is the major micro-vascular problem and chronic microvascular complication in diabetic patients and accounts for around half of all end-stage renal diseases globally [2]. DN is characterized by condensing of the glomerular basement membrane of both glomeruli and tubules, extracellular matrix and mesangial cell expansion with subsequent glomerular sclerosis, aggregation of extracellular matrix proteins in the mesangial interstitial space, and finally, glomerular damage which is the leading cause of microalbuminuria and renal failure [3-5]. Many factors such as genetic and hemodynamic factors, metabolic, oxidative stress, cytokine signaling pathways involvement, and inflammation are complicated in the pathogenesis and progression of DN [6]. Several therapy approaches are proposed for the management of diabetes and diabetes-related complications. Although pharmacological medication for type 2 diabetes in patients with normal renal function is limited to insulin, sulfonylureas, renin-angiotensin system blocking drugs, and metformin, these available therapies can slow but not inhibit DN development and severity of islet cells

depletion over time.[7, 8]. Thus, there is a need for enhanced therapeutic strategies that preserve normal renal function or slow down the progression of diabetic nephropathy.

To date, the administration of growth factors, cell therapies, platelet concentrates, and fresh whole blood transfusions have been used to treat diabetes. Emerging advanced therapies with cell-based and stem-cell-based modalities have shown exciting results for diabetes and diabetic complications, including DN [9, 10]. Mesenchymal stem cells (MSCs) are multipotent stem cells with self-renewal and multi-lineage differentiation capacity derived from various organs, including bone marrow, endometrial polyps, umbilical cord blood, and Wharton's jelly, menses blood and adipose tissue[11]. It has been shown that adipose-derived mesenchymal stem cells (ADSCs) have good plasticity and are ideal cell sources for tissue regeneration and homeostasis due to convenient access to the primary material, low immunogenicity, self-renewal, and multi-lineage differentiation capacity and their relative abundance [12].

Previous studies have reported that MSCs can migrate into injured kidney after systemic infusion, due to the inflammatory response in inflamed renal tissue [13]. Several characteristics play important roles in therapeutic features of MSCs, including triggering the activity of resident precursor cells, secretion of various growth factors, differentiation potency of MSCs to repair damaged tissue, modulation of inflammatory

and apoptotic state of the damaged local microenvironment in diseased tissue [14]. Recently, pre-conditioning and priming approaches have been used to improve the efficiency of MSCs-based therapies and various aspects of stem cell biology, including tethering, activation, and transmigration steps of systemic homing, anti-inflammatory, and anti-apoptotic efficiency [15]. Various preconditioning methods of MSCs and cell preconditioning with cytokines, growth factors, hypoxia, pharmacological agents, biomaterials, different chemicals, and genetically modified MSCs are suggested for different clinical applications and to optimize the efficacy of MSCs-based therapy [16]. Pre-conditioning of MSCs with pattern recognition receptors (PRRs) ligands has recently received more attention, and innate immune priming reduces chromatin resistance, which refers to epigenetic plasticity. TLRs are the major components of the innate immune system and play a significant role in MSC-mediated immune-regulatory functions [17, 18]. It's confirmed that, MSCs can be polarized into two diverse subtypes, MSC1 and MSC2, by activation of different Toll-like receptors (TLRs). This study aimed to investigate the capability of TLR4-primed MSCs to relieve DN in streptozotocin (STZ)-induced diabetic nephropathy rats and to examine the mechanisms underlying the protective effect of AD-MSCs in DN. Based on the mentioned data, we hypothesize that stem cell therapy by TLR4-primed MSCs has more advantages in reducing kidney damage in DN than MSCs alone.

Materials and Methods

Animals

A total of thirty healthy male Sprague-Dawley rats (6~7 weeks old, weighting 170-220 g) were included in this study and housed under standard pathogen-free conditions in standard cages and free access to standard with food and water "ad libitum" and were acclimated for one week under controlled temperature condition (23 ± 2 °C) and light controlled room. All experiments were conducted in agreement with international standards by animal welfare authorities.

Induction of diabetes type-1 and DN in rats

Rats were intraperitoneally injected with a single dose of streptozotocin (STZ: Sigma, St Louis, USA) at 55 mg/kg body weight, dissolved in cold sodium citrate buffer (0.1 M, pH 4.5) as described previously [19]. The normal control rat group (n=5) received an injection of a similar volume of phosphate-buffered saline (PBS). Three days after STZ administration, diabetes was confirmed when a random rat blood glucose level reading of more than 250 mg/dl. Blood glucose level (non-fast) was readily monitored using a portable glucometer on blood samples collected from the tail vein. Blood glucose was measured at different time intervals and considered as an index for hyperglycemia (data not shown). DN was established six weeks after the beginning of diabetes by calculating serum urea in blood and histopathological alterations scarifying one rat every week [20].

Animal groups and experimental design

The experimental groups were divided into six categories as follows: 0) Control group, which was injected intravenously with a single dose of PBS; 1) DN untreated group, which received intravenously with a single dose of STZ 55 mg/kg BW) dissolved in sodium citrate buffer (pH 4.5); 2) DN treated group, which received long-acting insulin (daily, subcutaneous injection, at the dose of 4 IU/200 g/day), following diabetes induction confirmation; 3) DN treated group, which received a single dose of 1×10^6 HFF cells), following diabetes induction confirmation; 4) DN treated group that receives a single pulse of 1×10^6 AD-MSCs), following diabetes induction confirmation; and 5) DN group that receives a single pulse of 1×10^6 TLR4-primed MSCs, following diabetes induction confirmation. All cell-based treated groups delivered the treatment by systemic intravenous injection into the tail vein. Insulin management was stopped 3 days before the terminal experiment.

Isolation of adipose tissue-derived mesenchymal stem cells (AT-MSCs)

Ad-SCs were derived from fat depots obtained from human lipoaspirates wastes. The adipose tissue was weighed and washed with cold PBS to remove red blood cells. Adipose tissue samples were digested for approximately 45 minutes at 37 °C with 1 mg collagenase type I and type-IV (Invitrogen) made in PBS and added 1% antibiotics and anti-mycotic agents. The collagenase cocktail activity was neutralized by adding 10% (v/v) fetal bovine serum (FBS) (Gibco). After centrifugation (300

g for 10 min), MSCs formed a pellet. Finally cells were transferred into Dulbecco's modified Eagle's medium (DMEM), Low glucose medium (DMEM-LG, Gibco) enriched in 10% FBS, 2mM L-glutamine (Gibco), and 1% antibiotic-antimycotic solution (Sigma Aldrich), in an incubator under a humidified air and 5% CO₂ atmosphere for 72 h at 37 °C. Suspended cells were omitted next day with medium changes and repeat this for every three days. This process was performed regularly and accurately until the adherent cells reached approximately 70-80% confluence before being released with 0.25 trypsin-Ethylenediaminetetraacetic acid (EDTA) and sub-cultured. The media was exchanged every three days, and the cells were passaged five times for use in this study.

Characterization of AD-MSCs by light microscopy and flow cytometry

AD-MSCs at day 14 were characterized by their adhesiveness and spindle shape cells between rounded cells by an inverted microscope (Olympus, Japan) to confirm the morphemically characteristics of AD-MSCs for confirming their identity. The surface antigen expression of AD-MSCs was confirmed by using flow cytometry. In order to assess the expression of MSC-related cell surface cluster of differentiation (CD) markers, the cells from the fourth passage were harvested by 0.25% trypsin containing 0.02% EDTA. In this regard, suspensions of AD-MSCs were harvested with trypsin/EDTA, and trypsin was neutralized by media containing 10% FBS and then suspended in 100 µl cold PBS.

Table 1. The list of antibodies used in flowcytometry experiments for the characterization of AD- Mesenchymal stem cells

| Antibody name | Company |
|---|---|
| Mouse anti-CD34 monoclonal antibody | Anti-CD34 antibody (IC0115): sc-7324, Santa Cruz Biotechnology, Inc. USA |
| Mouse anti-CD44 monoclonal antibody | Anti-HCAM antibody (F-4): sc-9960, Santa Cruz Biotechnology, Inc. USA |
| Mouse anti-CD45 monoclonal antibody | Anti-CD45 antibody (HIS24): sc-19615, Santa Cruz Biotechnology, Inc. USA |
| Mouse anti-CD73 monoclonal antibody | Anti-CD73 antibody (D-12): sc-398260, Santa Cruz Biotechnology, Inc. USA |
| Mouse anti-CD90 monoclonal antibody | Anti-Thy-1/CD90 antibody (a Thy-1A1): sc-53456, Santa Cruz Biotechnology, Inc. USA |
| Mouse anti-CD105 monoclonal antibody | Anti-Endoglin/CD105 antibody (P4A4): sc-20072, Santa Cruz Biotechnology, Inc. USA |
| Mouse anti-CD81 monoclonal antibody | CD81 monoclonal antibody (M38), PE: #A15781, Invitrogen, USA |
| Mouse anti-CD63 monoclonal antibody | Monoclonal Anti-CD63-FITC antibody produced in mouse, SAB4700217 Sigma Aldrich, Germany |
| Mouse anti-Vimentin monoclonal antibody | Anti-Vimentin Antibody (V9): sc-6260, Santa Cruz Biotechnology, Inc. USA |
| Goat anti-mouse IgG-FITC | Goat anti-mouse IgG-FITC: sc-2010, Secondary antibody, Santa Cruz Biotechnology, Inc. USA |

For cell-surface staining, cells were initially incubated in darkness for 1h at 4 °C with the following anti-human antibodies to characterize CD markers or isotype-matched control antibodies by MSCs (Table 1). Finally, cells were resuspended in 400 µl PBS and analyzed by a flow cytometer machine (BD Accuri™ C6), and the expression of the marker was quantified by using the Flowjo software 7.6.1 program. AD-MSCs express CD105, CD73, and CD29 on their surface and do not express CD34, or CD45.

Assaying multi-lineage differentiation potential of AD-MSCs

In order to characterize MSCs' multipotentiality, the multi-lineage differentiation potential of AD-MSCs was investigated. AD-MSCs could differentiate into osteogenic and adipogenic cells under different culture conditions. To induce differentiation into osteoblast and adipocytes, AD-MSCs (passage 4) were seeded at a density of 1.0×10^4 cells per well onto 6-well plates and cultured in osteogenic and

adipogenic medium for 3 weeks. All differentiation cultures included control cultures that receive common MSCs expansion medium. All cultured and negative control wells were done in triplicate wells for each condition, and medium exchange was performed twice a week. For osteogenic differentiation, after reaching 80% confluence, the complete medium was replaced with osteogenic differentiation medium including DMEM 10% FBS supplemented with 100 units/mL penicillin, 100 µg/mL streptomycin (Gibco), and 0.25 µg/mL fungizone, 0.1 µM dexamethasone, 50 µg/ml ascorbate-2-phosphate and 10 mM β- glycerophosphate (all from Sigma-Aldrich). Alkaline phosphatase activity and Alizarin Red S (Sigma Aldrich) staining for detecting calcium deposition were assessed on day 21 after induction. The adipogenic medium of differentiation is consisted of DMEM supplemented with 100 units/mL penicillin, 100 µg/mL streptomycin (Gibco), and 0.25

µg/mL fungizone 1 mM dexamethasone), 1 mg/ml insulin, 0.5 mM isobutylmethylxanthine (IBMX), 100 mM indomethacin (all from Sigma-Aldrich) and 10% FBS. Equal cell number was cultured in DMEM supplemented with 10% FBS for negative control. Media were changed every 3-4 days. Adipogenic differentiation was assessed by Oil red O (Sigma Aldrich) staining on day 21 after induction.

Pre-conditioning of AD-MSCs (TLR4 priming)

lipopolysaccharide (LPS, Sigma-Aldrich, MO) was used as the agonist for TLR4. In this study, AD-MSCs grown to 60-70% confluences were primed (treated) with LPS (10 ng/ml, TLR4-primed), in the culture medium (for 4 h). TLR4-agonist was supplemented to the fresh culture medium and incubated for 4 hours. Then cells were washed twice with 1 ml of media without the TLR-agonists. Following diabetes induction confirmation, ADSCs, TLR4-primed MSCs, and fibroblast were infused into rats intravenously.

Blood collection and tissue sampling

After 20 weeks of STZ administration, rats fasted, whole blood was obtained from their tail vein, and random glucose levels were measured using the portable glucometer. After a 16 h fast, for each animal, rats were euthanized, and after decapitation, both kidneys were immediately excised and weighted. The kidneys were quickly washed with PBS, and the cortex kidney tissues were removed quickly on ice and stored in liquid nitrogen for quantitative-real-time PCR analysis. Another part of the kidney cortex sample was immediately fixed for 1 day at room temperature in

formaldehyde (10%). Tissue samples were dehydrated with a graded series of alcohol, cleared in xylol, embedded in paraffin sections, and embedded in paraffin. Specimens were cut in a 4µm-thick section on a rotator microtome and mounted on a gelatin-coated glass slide. Coronal kidney sections (4 µm) were deparaffinized in xylene, rehydrated in decreasing concentrations of alcohol in water, and were stained with hematoxylin-eosin (HE) reagent (Sigma chemicals Co, St. Louis, MO) respectively, and observed under the light microscopy for evaluation of glomerular volume and glomerular mesangial expansion. The blood samples were saved, and serum samples were isolated for the assessment of blood urea nitrogen (BUN).

Evaluation of mRNA levels by real time polymerase chain reaction (RT-PCR)

Oligonucleotide primers were designed for the specific PCR amplification of a fragment of target genes. The primer sequences used for target genes are listed in table 2 for RT-PCR. Total RNA of MSCs and kidney tissues was isolated by Trizol reagent (Invitrogen) and treated with RNase-Free DNase I (Roche), according to the manufacturer's recommendations. The quality and quantity of the extracted RNA samples were qualified on a Nanodrop spectrophotometer (Thermo Scientific, USA).

1 µg total RNA was primed by an oligo (dT) primer through reverse transcription using RevertAid™ M-MuLV reverse transcriptase (Thermo Scientific, Germany) according to the supplier's recommendations. cDNA samples were standardized based on the content of β-actin cDNA as the housekeeping gene. β-actin cDNA was

evaluated by the performance of a β -actin PCR on multiple dilutions of each cDNA sample.

Real-time PCR

Real-time PCR reactions were performed using Eva-Green PCR Master mix (Solis bio dyne) and 80 nM of gene-specific forward and reverse primers as described above. The qRT-PCR reaction conditions were 95°C for 10 min, 95°C for 15 sec, 60°C for 20, and 72°C for 20 sec (40 cycles). Amplification and detection of target products were performed in triplicate in a StepOnePlus™ Real-Time PCR System (Life Technologies). Gene expression and expression levels of target genes were calculated as $2^{-\Delta\Delta(Ct)}$ [13], where Ct is cycle threshold, $\Delta\Delta(Ct) = \text{sample 1 } \Delta(Ct) - \text{sample 2 } \Delta(Ct)$; $\Delta(Ct) = \text{ACTB } (Ct) - \text{target gene } (Ct)$. Data were analyzed using Applied Biosystems software and GraphPad Prism software. Table 1. listed the primer sequence used for TLR4, NF-KB, BAX, Bcl2, caspase-3, tumor necrosis factor (TNF)- α , transforming growth factor (TGF)- β , and β -actin.

Evaluation of kidney function

In order to evaluate kidney function, blood urea was measured in various groups. BUN levels

were measured using an AccuABind enzyme-linked immunosorbent assay (ELISA) kit (Monobind, Inc. Lake Forest. USA). The assays were carried out according to the procedure described by the manufacturer's instructions.

Quantitative morphometric analysis of kidney tissue

Morphometric analysis was done via the Olympus imaging analysis system. Magnification of $\times 200$ is done for 25 randomly selected glomeruli, proximal, and distal convoluted tubules in each rat. Experiments were carried out according to the Guidelines for the Care and Use of Laboratory Animals (publication 86-23, revised in 1986; National Institutes of Health (NIH), Bethesda, MD, USA).

Statistical analysis

The statistical analysis was accomplished using a One-way analysis of variance and multiple comparison post hoc tests by Graph pad Prism5 software (GraphPad professional Prism). The results are presented as mean \pm SD, and a P-value less than 0.05 was considered statistically significant and highly significant when p-values were < 0.001 .

Table 2. Primer sequences used in Real-time RT-PCR experiments

| Gene | Strand | Primer sequence | PCR product size (bp) | Gene accession number |
|--|-----------|--------------------------------|-----------------------|-----------------------|
| <i>Actin-β</i> | Sense | 5'-CACACCCGCCACCAGTTC-3' | 166 | NM_031144.3 |
| | Antisense | 5'-GACCCATACCCACCATCACAC-3' | | |
| <i>Tumor necrosis factor-α</i> | Sense | 5'-CCAGACCCTCACACTCAGATCATC-3' | 84 | NM_012675.3 |
| | Antisense | 5'-TCCTCCGCTTGGTGGTTTGC-3' | | |
| <i>Transforming growth factor-β</i> | Sense | 5'-AGGGCTACCATGCCAACTTC-3' | 168 | NM_021578.2 |
| | Antisense | 5'-CCACGTAGTAGACGATGGGC-3' | | |
| <i>Caspase-3</i> | Sense | 5'-AGGCCGACTTCCTGTATGCT-3' | 223 | NM_012762.3 |
| | Antisense | 5'-GGCGCAAAGTGACTGGATGA-3' | | |
| <i>Caspase-8</i> | Sense | 5'-CCTCTGACCTCCGGTGTTTTA-3' | 200 | NM_022277.1 |
| | Antisense | 5'-CCAAGGGGTAGGAGAGCTGTA-3' | | |
| <i>B-cell lymphoma-2</i> | Sense | 5'-GGTGAAGTGGGGGAGGATTG-3' | 102 | NM_016993.2 |
| | Antisense | 5'-AGAGCGATGTTGTCCACCAG-3' | | |

Results

Characterization of AD-MSCs

The results of flow cytometry analysis of surface markers of the ADSCs isolated from the adipose tissues showed that the cells were positive for CD29 (91.9 %), CD44 (99.4 %), and CD105 (96.2 %); Whereas the cells were negative for CD45 (1.36 %) and CD34 (2.21 %) markers (Fig. 1). The ADSCs were further characterized after they were induced for osteogenic and adipogenic differentiation of ADSCs. Following differentiation, on day 21, the osteoblasts were indentified by their calcium deposits using Alizarin Red S stain. Accordingly, alkaline phosphatase activity was detected in the cells. In the case of adipogenic differentiation, the cells obtained on day 14, appeared with oil droplets stained with Oil-Red-O (Fig. 2).

LPS over expressed TLR4 in AD-MSCs

In the study, we typically used a TLR4-priming protocol that is defined as the incubation with LPS (10 ng/ml, 4 h) added as an agonist for TLR4. To confirm TLR4 priming, the expression of TLR4 was evaluated by qRT-PCR. Ad-MSCs preconditioning with LPS over-expressed TLR4 in mesenchymal stem cells in compared with untreated MSCs (Fig. 3).

Impact of TLR4-primed Ad-MSCs on blood urea nitrogen

The level of blood urea is an important indicator of kidney function. TLR4-primed MSCs administration in DN rats showed a significant decrease in urea level ($p < 0.0001$) as compared to other groups (Fig. 4).

Effect of TLR4-primed MSCs on TNF- α and TGF- β mRNA levels in kidney tissue

Diabetes mellitus and hyperglycemic conditions eventually lead to DN. In DN rats that received systemic HFF, the inflammatory cytokines such as TNF- α and TGF- β mRNA levels are elevated in kidney tissue in comparison to the normal control group. So, the mRNA levels of TNF- α and TGF- β showed a significant reduction in TLR4-primed MSCs groups (Figs. 5, 6).

The effect of TLR4-primed MSCs on apoptotic and inflammatory cell signaling components in renal tissue in DN

In diabetic conditions and DN, Bcl2 mRNA levels are down-regulated in renal tissue (Fig. 7). On the other hand, pro-apoptotic markers, including caspase-3 and caspase-8, are significantly over-expressed in DN and fibroblast groups (Figs. 8, 9). Administration of Ad-MSCs and TLR4-primed MSCs to DN in the T1-D rat model significantly increases in Bcl2 mRNA level and reverse the expression of pro-apoptotic markers, and down-regulates the expression of caspase-1, caspase-3, and caspase-8 (Figs. 7, 8 and 9).

Histological study

Hematoxylin and Eosin (H & E) staining

H&E stained sections of the control group exhibited normal glomeruli structure. Bowman's capsule generally consists of two distinct layers: visceral and parietal layers; tubular atrophy is a general term for chronic tubular damage with a thickened basement membrane [21]. Visceral and parietal cells of

glomeruli with normal Bowman’s space are separate in the control group (Fig. 10). H&E view of the DN exhibited that the glomeruli seemed to be deviated with extended Bowman’s space. Tubular atrophy was detected in proximal and distal tubules in cortex renal tissue, and blood vessels undergo considerable

thickening in DN condition (Fig. 10). H&E stained sections of the DN group that received a single pulse of 1×10^6 TLR4-primed MSCs showed significant improvement in renal structure compared to the other groups, as confirmed by histological studies.

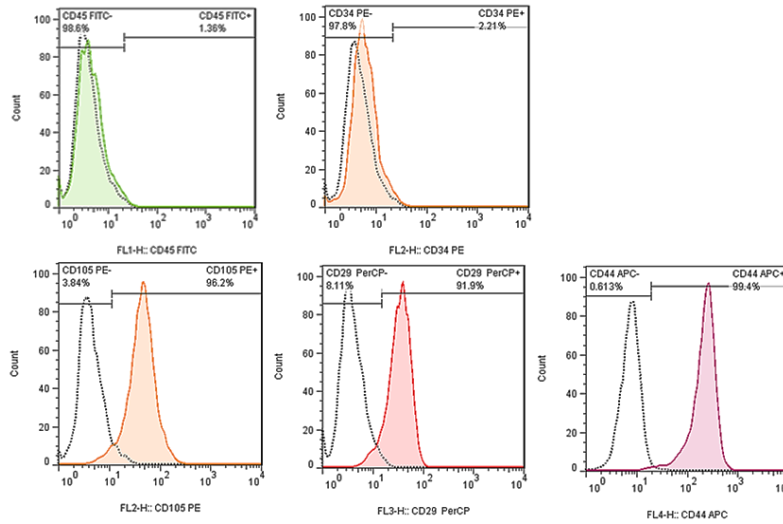


Fig. 1. Expression and confirmation of three classical cell surface markers expressed in adipose-derived mesenchymal stromal cells (AMSCs) by enzymatic digestion method were validated by flow cytometry among freshly isolated and expanded AMSCs. Illustrative histograms of surface marker expression compared to unstained AMSCs (negative control). ASCs expressed CD29, CD44, and CD90 but did not express CD34 and CD45. The percentage of positive cells for classical markers is assessed after the non-specific fluorescence signal was withdrawn with the isotype-matched control antibodies.

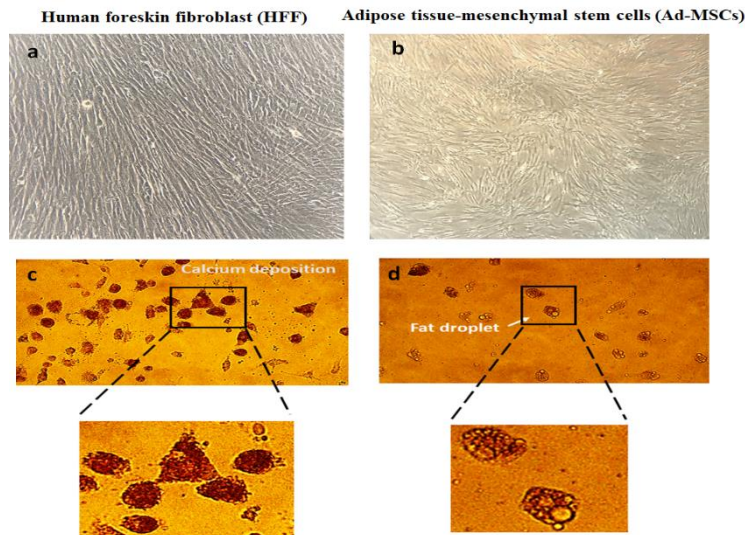


Fig. 2. Characterization of the adipose-derived mesenchymal stem cells (AD-MSCs) (a) and human foreskin fibroblast (b) in culture, differentiation potency: Cultured cells show fibroblast-like morphology (a). Alizarin red staining and alkaline phosphatase detection show cells grown in a defined inductive medium differentiate into osteogenic lineages (c). Oil red O staining shows cells grown in the defined inductive medium differentiate into adipogenic lineages (d).

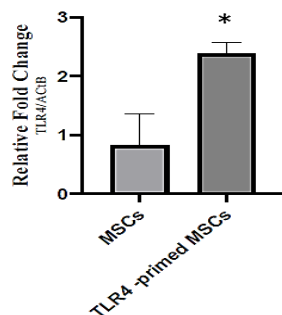


Fig. 3. Toll-like receptor 4 (TLR4) expression in adipose-derived mesenchymal stem cells (AD-MSCs) after pre-conditioning with lipopolysaccharides. Data are representative of triplicate measurements. * Comparison: Mesenchymal stem cells (MSCs) Vs. TLR4-primed MSCs. Error bars indicate SD. * p-value < 0.001 comparison to unprimed MSCs.

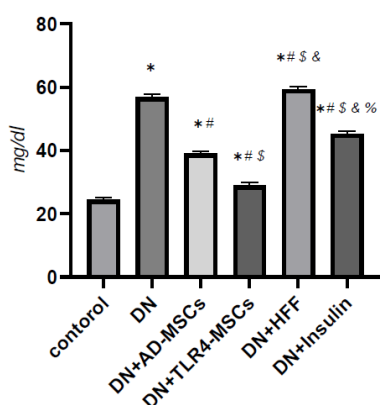


Fig. 4. Blood Urea Nitrogen (BUN) assessment in the different studied rat's groups. The results represented the means \pm SD of two independent experiments (n = 5). * Comparison: Control Vs. diabetic nephropathy (DN), mesenchymal stem cells (MSCs), Toll-like receptor 4 (TLR4)-primed MSCs, Insulin, Fibroblasts. # Comparison: DN Vs. MSCs, TLR4-primed MSCs, Insulin, Fibroblasts. \$ Comparison: MSCs Vs. TLR4-primed MSCs, Insulin, Fibroblasts. & Comparison: TLR4-primed MSCs Vs. Insulin, Fibroblasts. % Comparison: Insulin Vs. Fibroblasts.

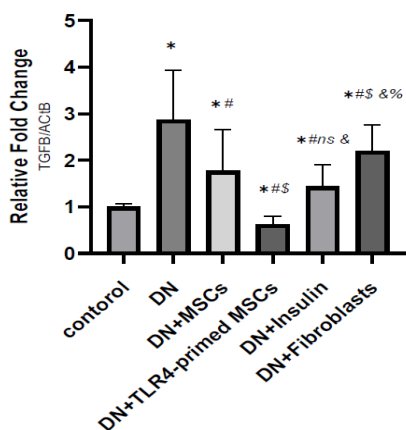


Fig. 5. Relative mRNA level of transforming growth factor (TGF)- β in different experimental groups. This relative mRNA level was identified by quantitative RT-PCR in kidney tissues from the control, diabetic nephropathy (DN), DN-insulin, DN-fibroblast, DN- mesenchymal stem cells (MSCs) and DN-TLR4-primed MSCs groups. The results represented the means \pm SD of two independent experiments (n = 5). * Comparison: Control Vs. DN, MSCs, Toll-like receptor 4(TLR4)-primed MSCs, Insulin, Fibroblasts. # Comparison: DN Vs. MSCs, TLR4-primed MSCs, Insulin, Fibroblasts. \$ Comparison: MSCs Vs. TLR4-primed MSCs, Insulin, Fibroblasts. & Comparison: TLR4-primed MSCs Vs. Insulin, Fibroblasts. % Comparison: Insulin Vs. Fibroblasts.

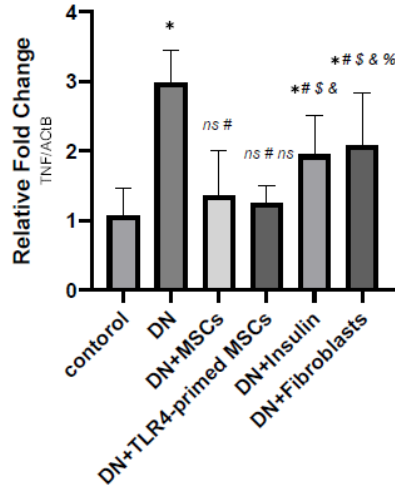


Fig. 6. Relative mRNA level of tumor necrosis factor (TNF)-α in different experimental groups. This relative mRNA level was identified by quantitative RT-PCR in kidney tissues from the control, diabetic nephropathy (DN), DN-insulin, DN-fibroblast, DN- mesenchymal stem cells (MSCs), and DN-Toll-like receptor 4(TLR4)-primed MSCs groups. The results represented the means ± SD of two independent experiments (n = 5). * Comparison: Control Vs. DN, MSCs, TLR4-primed MSCs, Insulin, Fibroblasts. # Comparison: DN Vs. MSCs, TLR4- primed MSCs, Insulin, Fibroblasts. \$ Comparison: MSCs Vs. TLR4- primed MSCs Insulin, Fibroblasts. & Comparison: TLR4- primed MSCs Vs. Insulin, Fibroblasts. % Comparison: Insulin Vs. Fibroblasts.

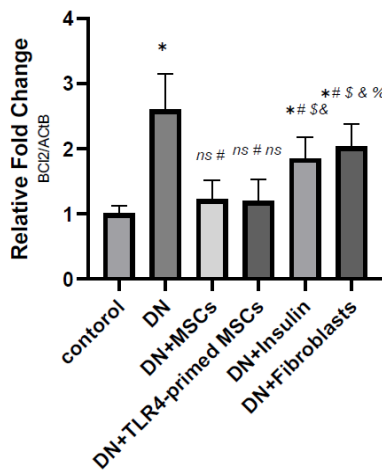


Fig. 7. Relative mRNA level of Bcl₂ in different experimental groups. This relative mRNA level was identified by quantitative RT-PCR in kidney tissues from the control, diabetic nephropathy (DN), DN-insulin, DN-fibroblast, DN- mesenchymal stem cells (MSCs) and DN- Toll-like receptor 4(TLR4)-primed MSCs groups. The results represented means ± SD of two independent experiments (n = 5). * Comparison: Control Vs. DN, MSCs, TLR4-primed MSCs, Insulin, Fibroblasts. # Comparison: DN Vs. MSCs, TLR4- primed MSCs, Insulin, Fibroblasts. \$ Comparison: MSCs Vs. TLR4- primed MSCs Insulin, Fibroblasts. & Comparison: TLR4- primed MSCs Vs. Insulin, Fibroblasts. % Comparison: Insulin Vs. Fibroblasts.

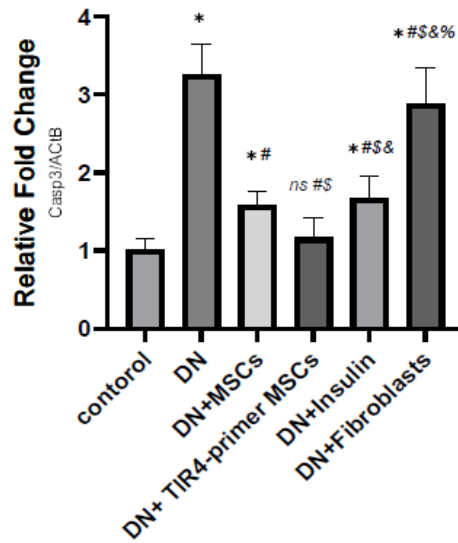


Fig. 8. Relative mRNA level of caspase-3 in different experimental groups. This relative mRNA level was identified by quantitative RT-PCR in kidney tissues from the control, diabetic nephropathy (DN), DN-insulin, DN-fibroblast, DN-mesenchymal stem cells (MSCs) and DN-Toll-like receptor 4(TLR4)-primed MSCs groups. The results represented the means \pm SD of two independent experiments (n = 5). * Comparison: Control Vs. DN, MSCs, TLR4-primed MSCs, Insulin, Fibroblasts. # Comparison: DN Vs. MSCs, TLR4-primed MSCs, Insulin, Fibroblasts. \$ Comparison: MSCs Vs. TLR4-primed MSCs Insulin, Fibroblasts. & Comparison: TLR4-primed MSCs Vs. Insulin, Fibroblasts. % Comparison: Insulin Vs. Fibroblasts.

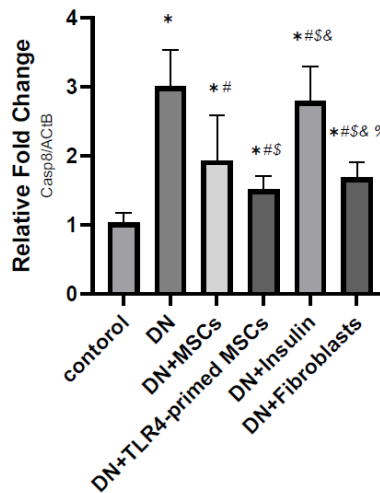


Fig. 9. Relative mRNA level of caspase-8 in different experimental groups. This relative mRNA level was identified by quantitative RT-PCR in kidney tissues from the control, diabetic nephropathy (DN), DN-insulin, DN-fibroblast, DN-mesenchymal stem cells (MSCs) and DN-Toll-like receptor 4(TLR4)-primed MSCs groups. The results represented the means \pm SD of two independent experiments (n = 5). * Comparison: Control Vs. DN, MSCs, TLR4-primed MSCs, Insulin, Fibroblasts. # Comparison: DN Vs. MSCs, TLR4-primed MSCs, Insulin, Fibroblasts. \$ Comparison: MSCs Vs. TLR4-primed MSCs Insulin, Fibroblasts. & Comparison: TLR4-primed MSCs Vs. Insulin, Fibroblasts. % Comparison: Insulin Vs. Fibroblasts.

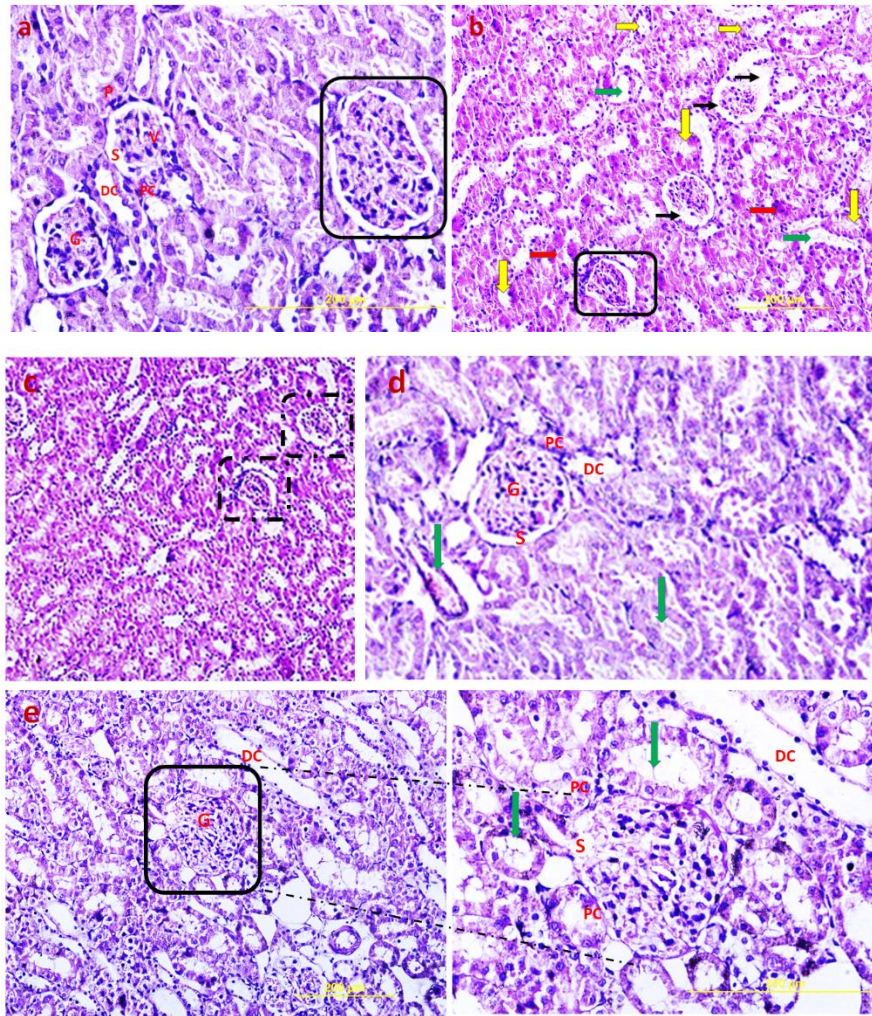


Fig. 10. H&E staining from renal cortex sections at magnification $\times 200$. **a:** As indicates in figure, typical structure is showed in nephron structure. Glomeruli (G) with Bowman's spaces (S) which is lined by visceral (V) and parietal (P) cells are presented. **b:** Diabetic nephropathy rat is confirmed by distorted glomeruli and expansion of Bowman space and little size in compared with normal rats (atrophy of glomerulus). Some tubules are atrophied (yellow curve), destroyed (red curve) and some of them are dilated (green curve). Increase of an amorphous, eosinophilic, glassy substance within the vascular wall is observed in blood vessels (hyalinization) (Vertical yellow curve). **c:** Fibroblast group shows distorted and contracted glomeruli (dashes lines). **d** and **e:** Mesenchymal stem cells (MSCs) (d) and Toll-like receptor 4-primed MSCs (e) groups shows marked enlargement in the glomeruli structures. The glomeruli (G), proximal tubules (PC), and distal tubules (DC) seem approximately like to that of the control. Blood vessels have a normal and large structure (Vertical green curve).

Discussion

Currently, diabetic nephropathy is the major cause of renal disorders in developed countries [22]. Although the etiology of these complications is not well understood, both hyperglycemia and hypertension are considered to be the main causes of renal injury in diabetes. Streptozotocin has been proposed to induce

diabetic animal models and other related complications. Streptozotocin, a glucosamine-nitrosourea compound, is a β cell-specific toxin that influences permanent damage to pancreatic beta cells through free radicals, nitric oxide generation, and DNA damage [23, 24].

Recently, MSCs-based cell therapy takes a potential treatment for diabetes and DN. A recent meta-analysis and systematic reviews reported that MSCs might improve blood glucose and reduce serum creatinine (SCr) and BUN [25]. On the other hand, MSCs are potent in blood glucose reduction through beta cell function recovery and regulate inflammatory processes, fibrosis and angiogenesis, and podocyte protection [26, 27].

ADSCs are now a good source of mesenchymal stem cells due to their ability to promote proliferation and differentiation into various cell lineage [28]. The use of AD-MSCs in cell therapies is attractive because of their easy accessibility and isolation, multi-lineage differentiation, low expression of co-stimulatory molecules and immunosuppressive properties, immunomodulation capacity, evoke only minimal immune responses, low immunogenicity and anti-inflammatory effects [29, 30].

TLRs are components of pattern recognition receptors that initiate the innate immune responses to exogenous molecules that are named pathogen-associated molecular patterns and endogenous signals that are derived from injured tissues (damage-associated molecular patterns, or DAMPs) [31]. The expression patterns of TLRs in various cell types, especially MSCs, from different sources have been estimated in several studies. In this regard, the expression of mRNAs for TLR2, TLR3, TLR4, and TLR9 in AD-MSCs is confirmed [32, 33]. On the other hand, TLRs agonist influence the epigenetic plasticity of MSCs and the over-expressed cell surface ligand that

contributes to stem cell recruitment, migration, and homing of stem cells [34-36].

It has been shown that modulating TLR signaling can alter MSC phenotype and immunomodulation properties [37]. Indeed, MSCs can be “polarized” by TLR priming into distinct immunomodulatory phenotypes. TLR4 priming leads to an immune-activating MSC-1 phenotype which is named the pro-inflammatory state [38]. Recent studies indicated that mild inflammation needs regeneration in injured tissues. As mentioned in a previous study, the potency of cardiac regeneration of TLR4-primed MSCs in myocardial infarction is confirmed [39]. Up to now, it has not been reported that the effect of preconditioning of MSCs with innate immune agonists, including TLRs agonists, in the treatment of DN. The effects of TLR stimulation on the efficiency of MSCs on DN treatment using TLR4 agonists as a key component of the innate immune system have not been completely elucidated until now. This study aimed to examine the anti-inflammatory and anti-apoptotic properties of pre-conditioned MSCs with TLR4 agonies, LPS, to improve the renal parameters and function in the DN rat model. Due to fibroblasts sharing the same morphology as MSCs and expressing the identical cell surface antigens as MSCs [40], human fibroblast foreskin cells served as the negative control for MSCs to display the unique therapeutic effects of MSCs independent of similar spindle-like morphology.

Kidney function analysis showed a substantial decrease in serum urea level in MSCs and TLR-

4-primed MSCs groups compared with other groups. This result indicates that renal function was an improved and better outcome. The histological analysis shows that the kidney of DN groups undergoes mesangial matrix expansion, thickening of the glomerular basement, arteriolar hyalinosis, and nodular glomeruli with expanded Bowman's space. These findings are similar to previous studies that reported histological changes and glomerular basement membrane thickening [41]. Other studies confirmed histological abnormalities in renal tissue such as thickening of tubular basement membrane, glomerulosclerosis, loss of brush border of proximal tubules, tubular atrophy, and proliferation of the mesangial cell and mesangial expansion [42-44]. Fibroblast administration has no instructive impact on structural abnormalities of the kidney seen in DN, and no improvement of morphological outcomes in DN. The histological analysis demonstrated that TLR4-primed MSCs injection had stronger effects than un-primed MSCs and significantly restored histological parameters to the control level. In fact, the microscopic histological view of the renal tissue after injection of LPS-primed MSCs in the DN group showed regular renal corpuscles and renal tubules. This result is consistent with other related studies emphasizing that MSCs can regenerate and protect mesangial cells [45]. MSCs have a renotropic protective effect and can be reduced inflammation and fibrosis in damaged DN [46, 47]. TLR4-primed MSCs improved the recovery of renal function in DN, proposing that LPS-

primed MSCs contribute to reform in cytokine production [48]. TGF- β 1 is a fibrogenic growth factor formed in the renal parenchymal tissue in response to injury or inflammation and plays a vital role in progressive renal atrophy by triggering apoptosis in the endothelial cells and collagen accumulation [49, 50]. In this study, the expression of TGF- β in DN was modulated by MSCs and TLR4-primed MSCs. These results were verified by qRT-PCR for TGF- β results in DN groups and decreased in MSCs and TLR4-primed MSCs groups. These results suggested that MSCs and TLR4-primed MSCs can inhibit inflammation-mediated fibrosis and down-regulate inflammation-related TGF- β expression in renal tissue in DN. Another pro-inflammatory cytokine was TNF- α . TNF- α can activate the extrinsic apoptosis signaling pathway and trigger kidney epithelial cells to release chemo-attractive factors. On the other hand, TNF- α increases the production of RNS and ROS, disrupting the glomerular capillary integrity and causing the secretion of protein in urine [51]. Besides, TNF- α contributes to caspase-3-independent apoptosis in various cells [52]. MSCs or TLR4-primed MSCs infusion in DN reduces the mRNA levels of TNF- α in compared to another experimental group. TNF- α activates the intrinsic and extrinsic programmed cell death and triggers the caspase family, especially caspase-8. Caspase-8 in the pathways of type-1, activates effector caspases (caspase-3, -6, and -7) and stimulates apoptosis. Caspase-8, via the intrinsic apoptosis cell signaling pathway, promotes cell death depending on mitochondria pathways that mediate by Bcl2 protein in the

mitochondria [53]. The recent study confirmed a significant increase in TNF- α , caspase-3, and caspase-8 mRNA levels in DN compared to the control group. MSCs and TLR-4-primed MSCs inhibit TNF- α apoptotic pathway by weakening TNF- α , caspase-3, and caspase-8 mRNA levels in the DN model.

On the other hand, when the ratio of Bax/Bcl-2 is raised, the protective and defensive effects of Bcl-2 are disturbed. In our study, we establish the increased expression of Bcl-2 in MSCs and TLR4-primed MSCs therapy of DN. It seems that the elevated expression of Bcl-2 mediated by MSCs administration has protective effects on renal epithelial cells and inhibits renal cell apoptosis and fibrosis.

Conclusion

Priming with LPS enhances the therapeutic effects of MSCs on DN. MSC and TLR4-primed MSCs diminished DN pathogenesis, supporting the hypothesis that MSCs and alarmed-MSCs may exert a protective effect on

damaged tissue such as inflamed diabetic kidneys. Our results proposed that MSCs priming with innate immune agonists such as TLR4 improve the efficiency of MSCs-based therapy in DN. Indeed, TLR4-primed MSCs administration enhances kidney regeneration and reduces the expression of pro-inflammatory mediators that elevate the regenerative capacity of renal tissue and alleviate renal fibrosis. It is thought that pre-conditioning of MSCs with TLR4 agonist, LPS, and TLR4-primed MSCs administration might be a potential treatment for DN. MSCs-based cell therapy and pre-conditioning approaches suggest a hopeful future for DN treatment. However, more pre-clinical studies are required to identify the efficacy of primed-based MSCs in DN in order to translate them into clinical approaches.

Conflict of Interest

The authors declare no competing interests.

Acknowledgment

This work was supported by Yazd Cardiovascular Research Center (YCRC).

References

- [1]. Giri B, Dey S, Das T, Sarkar M, Banerjee J, Dash SK. Chronic hyperglycemia mediated physiological alteration and metabolic distortion leads to organ dysfunction, infection, cancer progression and other pathophysiological consequences: an update on glucose toxicity. *Biomedicine & Pharmacotherapy* 2018; 107: 306-28.
- [2]. Donate-Correa J, Luis-Rodríguez D, Martín-Núñez E, Tagua VG, Hernández-Carballo C, Ferri C, et al. Inflammatory targets in diabetic nephropathy. *Journal of Clinical Medicine*.2020; 9(2): 458.
- [3]. Soldatos G, Cooper M. Diabetic nephropathy: important pathophysiologic mechanisms. *Diabetes Research and Clinical Practice* 2008; 82(S 1): 75-9.
- [4]. Marshall CB. Rethinking glomerular basement membrane thickening in diabetic nephropathy: adaptive or pathogenic? *Am J Physiol Renal Physiol*. 2016; 311(5): 831-43.
- [5]. Brosius FC. New insights into the mechanisms of fibrosis and sclerosis in diabetic nephropathy. *Rev Endocr Metab Disord* 2008; 9(4): 245-54.
- [6]. Forbes J, Fukami K, Cooper M. Diabetic nephropathy: where hemodynamics meets metabolism. *Experimental and Clinical Endocrinology & Diabetes* 2007; 115(2): 69-84.
- [7]. Cernes R, Zimlichman R. Diabetes mellitus type 2 and proteinuria. *Type* 2013; 2: 205-31.
- [8]. Burney BO, Kalaitzidis RG, Bakris GL. Novel therapies of diabetic nephropathy. *Current Opinion in Nephrology and Hypertension* 2009; 18(2): 107-11.
- [9]. Hamad FRB, Rahat N, Shankar K, Tsouklidis N. Efficacy of stem cell application in diabetes

- mellitus: promising future therapy for diabetes and its complications. *Cureus* 2021; 13(2): 13563.
- [10]. Qi Y, Ma J, Li S, Liu W. Applicability of adipose-derived mesenchymal stem cells in treatment of patients with type 2 diabetes. *Stem Cell Research & Therapy* 2019; 10(1): 1-13.
- [11]. Ding DC, Shyu WC, Lin SZ. Mesenchymal stem cells. *Cell Transplant* 2011; 20(1): 5-14.
- [12]. Guo X, Huang D, Li D, Zou L, Lv H, Wang Y, et al. Adipose-derived mesenchymal stem cells with hypoxic preconditioning improve tenogenic differentiation. *J Orthop Surg Res.* 2022; 17(1): 49.
- [13]. Morigi M, Imberti B, Zoja C, Corna D, Tomasoni S, Abbate M, et al. Mesenchymal stem cells are renotropic, helping to repair the kidney and improve function in acute renal failure. *Journal of the American Society of Nephrology* 2004; 15(7): 1794-804.
- [14]. Togel F, Weiss K, Yang Y, Hu Z, Zhang P, Westenfelder C. Vasculotropic, paracrine actions of infused mesenchymal stem cells are important to the recovery from acute kidney injury. *American Journal of Physiology-Renal Physiology* 2007; 292(5): 1626-635.
- [15]. De Becker A, Van Riet I. Homing and migration of mesenchymal stromal cells: how to improve the efficacy of cell therapy? *World Journal of Stem Cells* 2016; 8(3): 73.
- [16]. Noronha NC, Mizukami A, Caliári-Oliveira C, Cominal JG, Rocha JLM, Covas DT, et al. Priming approaches to improve the efficacy of mesenchymal stromal cell-based therapies. *Stem Cell Res Ther.* 2019; 10(1): 131.
- [17]. Rivera-Cruz CM, Figueiredo ML. Polarization of adipos-derived mesenchymal stem/stromal cells via Toll-like receptor priming and potential synergy with interleukin- 27 delivery. *The FASEB Journal* 2020; 34(S1): 1-10.
- [18]. Yan H, Wu M, Yuan Y, Wang ZZ, Jiang H, Chen T. Priming of toll-like receptor 4 pathway in mesenchymal stem cells increases expression of B cell activating factor. *Biochemical and Biophysical Research Communications* 2014; 448(2): 212-17.
- [19]. Qiao Y, Gao K, Wang Y, Wang X, Cui B. Resveratrol ameliorates diabetic nephropathy in rats through negative regulation of the p38 MAPK/TGF- β 1 pathway. *Exp Ther Med.* 2017; 13(6): 3223-230.
- [20]. Fang Y, Tian X, Bai S, Fan J, Hou W, Tong H, et al. Autologous transplantation of adipose-derived mesenchymal stem cells ameliorates streptozotocin-induced diabetic nephropathy in rats by inhibiting oxidative stress, pro-inflammatory cytokines and the p38 MAPK signaling pathway. *International Journal of Molecular Medicine* 2012; 30(1): 85-92.
- [21]. Murray I, Paolini MA. Histology, kidney and glomerulus. *statpearls. treasure island (FL): StatPearls Publishing Copyright © 2022, StatPearls Publishing LLC; 2022.*
- [22]. Kim KS, Lee JS, Park JH, Lee EY, Moon JS, Lee SK, et al. Identification of novel biomarker for early detection of diabetic nephropathy. *Biomedicines* 2021; 9(5): 457.
- [23]. Motyl K, McCabe LR. Streptozotocin, type I diabetes severity and bone. *Biological Procedures Online* 2009; 11(1): 296-315.
- [24]. Tonne JM, Sakuma T, Deeds MC, Munoz-Gomez M, Barry MA, Kudva YC, et al. Global gene expression profiling of pancreatic islets in mice during streptozotocin-induced β -cell damage and pancreatic Glp-1 gene therapy. *Disease Models & Mechanisms* 2013; 6(5): 1236-245.
- [25]. Lin W, Li H-Y, Yang Q, Chen G, Lin S, Liao C, et al. Administration of mesenchymal stem cells in diabetic kidney disease: a systematic review and meta-analysis. *Stem Cell Research & Therapy* 2021; 12(1): 1-21.
- [26]. Shi Y, Wang Y, Li Q, Liu K, Hou J, Shao C, et al. Immunoregulatory mechanisms of mesenchymal stem and stromal cells in inflammatory diseases. *Nature Reviews Nephrology* 2018; 14(8): 493-507.
- [27]. Wang Y, Shan SK, Guo B, Li F, Zheng MH, Lei LM, et al. The multi-therapeutic role of MSCs in diabetic nephropathy. *Frontiers in Endocrinology* 2021(678): 671566.
- [28]. Ma T, Sun J, Zhao Z, Lei W, Chen Y, Wang X, et al. A brief review: adipose-derived stem cells and their therapeutic potential in cardiovascular diseases. *Stem Cell Research & Therapy* 2017; 8(1): 124.
- [29]. Locke M, Windsor J, Dunbar PR. Human adipose- derived stem cells: isolation, characterization and applications in surgery. *Journal of Surgery* 2009; 79(4): 235-44.
- [30]. Lukomska B, Stanaszek L, Zuba-Surma E, Legosz P, Sarzynska S, Dreka K. Challenges and controversies in human mesenchymal stem cell therapy. *Stem Cells International* 2019; 2019.
- [31]. Tsan MF, Gao B. Endogenous ligands of Toll-like receptors. *Journal of Leukocyte Biology* 2004; 76(3): 514-19.
- [32]. Wang S, Li X, Zhao RC. Transcriptome analysis of long noncoding RNAs in Toll-like receptor 3-activated mesenchymal stem cells. *Stem Cells International* 2016; 2016.
- [33]. Rizvanov AA, Persson J, Şahin F, Bellusci S, Oliveira PJ. Hematopoietic and mesenchymal stem cells in biomedical and clinical applications. *Hindawi*; 2016.
- [34]. Najjar M, Krayem M, Meuleman N, Bron D, Lagneaux L. Mesenchymal stromal cells and toll-like receptor priming: a critical review. *Immune Network* 2017; 17(2): 89-102.

- [35]. Sallustio F, Curci C, Stasi A, De Palma G, Divella C, Gramignoli R, et al. Role of toll-like receptors in actuating stem/progenitor cell repair mechanisms: different functions in different cells. *Stem Cells International* 2019; 2019.
- [36]. de Cássia Noronha N, Mizukami A, Caliári-Oliveira C, Cominal JG, Rocha JLM, Covas DT, et al. Priming approaches to improve the efficacy of mesenchymal stromal cell-based therapies. *Stem Cell Research & Therapy* 2019; 10(1): 1-21.
- [37]. DelaRosa O, Dalemans W, Lombardo E. Toll-like receptors as modulators of mesenchymal stem cells. *Frontiers in Immunology* 2012; 3: 182.
- [38]. Waterman RS, Tomchuck SL, Henkle SL, Betancourt AM. A new mesenchymal stem cell (MSC) paradigm: polarization into a pro-inflammatory MSC1 or an immunosuppressive MSC2 phenotype. *PloS one* 2010; 5(4): 10088.
- [39]. Yao Y, Zhang F, Wang L, Zhang G, Wang Z, Chen J, et al. Lipopolysaccharide preconditioning enhances the efficacy of mesenchymal stem cells transplantation in a rat model of acute myocardial infarction. *Journal of Biomedical Science* 2009; 16(1): 1-11.
- [40]. Denu RA, Nemcek S, Bloom DD, Goodrich AD, Kim J, Mosher DF, et al. Fibroblasts and mesenchymal stromal/ stem cells are phenotypically indistinguishable. *Acta Haematol.* 2016; 136(2): 85-97.
- [41]. Najafian B, Alpers CE, Fogo AB. Pathology of human diabetic nephropathy. *Diabetes and Kidney* 2011; 170: 36-47.
- [42]. Raparia K, Usman I, Kanwar YS. Renal morphologic lesions reminiscent of diabetic nephropathy. *Archives of Pathology & Laboratory Medicine* 2013; 137(3): 351-59.
- [43]. Zafar M, Naqvi S, Ahmed M, Kaimkhani ZA. Altered kidney morphology and enzymes in streptozotocin induced diabetic rats. *Int J Morphol.* 2009; 27(3): 783-90.
- [44]. Fioretto P, Steffes MW, Mauer M. Glomerular structure in nonproteinuric IDDM patients with various levels of albuminuria. *Diabetes* 1994; 43(11): 1358-364.
- [45]. Wong CY, Cheong SK, Mok PL, Leong CF. Differentiation of human mesenchymal stem cells into mesangial cells in post-glomerular injury murine model. *Pathology* 2008;40(1):52-7.
- [46]. Park JH, Hwang I, Hwang SH, Han H, Ha H. Human umbilical cord blood-derived mesenchymal stem cells prevent diabetic renal injury through paracrine action. *Diabetes Research and Clinical Practice* 2012; 98(3): 465-73.
- [47]. Lv SS, Liu G, Wang JP, Wang WW, Cheng J, Sun AL, et al. Mesenchymal stem cells transplantation ameliorates glomerular injury in streptozotocin-induced diabetic nephropathy in rats via inhibiting macrophage infiltration. *International Immunopharmacology* 2013; 17(2): 275-82.
- [48]. Chishti AS, Sorof JM, Brewer ED, Kale AS. Long-term treatment of focal segmental glomerulosclerosis in children with cyclosporine given as a single daily dose. *American Journal of Kidney Diseases* 2001; 38(4): 754-60.
- [49]. Tunçdemir M, Öztürk M. The effects of angiotensin-II receptor blockers on podocyte damage and glomerular apoptosis in a rat model of experimental streptozotocin-induced diabetic nephropathy. *Acta Histochemica* 2011; 113(8): 826-32.
- [50]. Kim KK, Sheppard D, Chapman HA. TGF- β 1 Signaling and Tissue Fibrosis. *Cold Spring Harb Perspect Biol.* 2018; 10(4): 22293.
- [51]. Koike N, Takamura T, Kaneko S. Induction of reactive oxygen species from isolated rat glomeruli by protein kinase C activation and TNF- α stimulation, and effects of a phosphodiesterase inhibitor. *Life Sciences* 2007; 80(18): 1721-728.
- [52]. Alvarez S, Blanco A, Fresno M, Muñoz-Fernández MÁ. TNF- α contributes to caspase-3 independent apoptosis in neuroblastoma cells: role of NFAT. *PloS one* 2011; 6(1): 16100.
- [53]. Luo X, Budihardjo I, Zou H, Slaughter C, Wang X. Bid, a Bcl2 interacting protein, mediates cytochrome c release from mitochondria in response to activation of cell surface death receptors. *Cell* 1998; 94(4): 481-90.